Kinome-wide RNAi Screening to Identify Kinases Involved in Post-translational Modification of FUS

Serena E. B. Liu

Thesis submitted to the
Faculty of Graduate and Postdoctoral Studies
In partial fulfillment of the requirements for the degree of
Master of Science in Biochemistry

Department of Biochemistry, Microbiology and Immunology
Faculty of Medicine
University of Ottawa

Abstract

Amyotrophic lateral sclerosis (ALS) is a devastating adult onset neurodegenerative disorder characterized by the selective degeneration of upper and lower motor neurons. Patients typically die from respiratory failures within 2-5 years after diagnosis. One of the milestones in ALS research is the discovery Fused in Sarcoma (FUS), an ALS causative gene. FUS is an RNA/DNA-binding protein and predominantly resides in the nucleus. Majority of the FUS mutations are located in the C-terminus and causing aberrant misdistribution to the cytoplasm. Currently, only a few binding partners of FUS are known, which makes it difficult to speculate on the function and interaction of the protein. In this study, we conducted a kinome-wide RNAi screen to identify kinases that affect the localization of FUS. A dual specificity protein kinase named CDC2-like kinase (CLK1) from screen was found to be responsible for in post-translational modification of FUS and affects the localization of FUS in the nucleus. The identification of CLK1 as FUS-modifying kinase is consistent with roles ascribed to both in the binding and regulation of RNA.

Acknowledgments

Foremost, I would like to express my sincere appreciation and gratitude to my supervisor Dr. Douglas Gray for the continuous support of my graduate study and research. Without his guidance and constant help, this thesis would not have been possible.

I would like to thank my thesis committee members, Dr. John Woulfe, and Dr. Robert Screaton for serving as my committee members and sharing their insightful comments and in-depth knowledge on my work.

Thanks are also due to the friendship and support I have received from members of the Gray-Woulfe Lab (especially Josée, Madison, and Mei), and members of the Screaton Lab (especially Qiujiang and Stephen).

I would also like to thank all the friends who supported me in writing and incented me to strive towards my goal.

Lastly, a special thanks to my family, Mom and Dad, for their unwavering support and interest.

Table of Contents

List of Abbreviations

ALS	Amyotrophic lateral sclerosis
Brk	Breast tumor kinase
BSA	Bovine Serum albumin
CLK1	CDC2-like kinase
CLK1_Mix	All four CLK1 siRNAs (CLK1_1, CLK1_2, CLK1_5, CLK1_6)
CNT	Control
EWS	Ewing's sarcoma
FUS	Fused in sarcoma
hnRNP	Heterogeneous nuclear ribonucleoprotein
IF	Immunofluorescence
IP	Immunoprecipitation
PBS	phosphate-buffered saline pH7.4
pS	Phosphoserine
pY	Phosphotyrosine
RNAi	RNAi interference
Sam68	Src-Associated substrate in Mitosis of 68 kDa
Ser	Serine
siRNA	Small inferring RNA
SKOV3	Human ovarian carcinoma cell line
TBST	Tris buffered saline with Tween® 20
Thr	Threonine

Trn1	Transportin 1
Trn	Transportin 1&2
TX-100	Triton X-100
Tyr	Tyrosine
U2OS	Human osteosarcoma cell line
U87MG	Human glioblastoma cell line

List of Figures

List of Tables

Chapter 1: Introduction

1. Amyotrophic lateral sclerosis

The name, Amyotrophic Lateral Sclerosis has a Greek root. *Amyotrophic* means no muscle nourishment. *Lateral* refers to the location of the affected neurons in the spinal cord, the degeneration of which results in hardening or *Sclerosis.* In the United States, it is also known as Lou Gehrig's disease, after the baseball legend Lou Gehrig who passed away by the disease in the late 1930s.

Amyotrophic lateral sclerosis (ALS) is an adult onset neurodegenerative disorder characterized by the selective degeneration of upper and lower motor neurons. The disease results in the wasting of muscles and permanent paralysis; however, oculomotor, sensory, and autonomic functions are not affected. Most patients die from respiratory failure within 2-5 years after the initial onset of symptoms (Iguchi et al.). No treatment is available for reversing the course of ALS, but there are therapies offering to slow down the progression of the disease and prevent unnecessary complications for the patients.

ALS can be classified into two general categories, sporadic and familial. Approximately 90% of all cases of ALS are sporadic, and the remainder is familial. Familial ALS (fALS) is usually inherited in an autosomal dominant manner, and in some cases, it is X-linked. The discrimination between familial and sporadic ALS is difficult and varies on the definition of familial that is applied. By strict definition for familial ALS, at least one first or second-degree relative of the affected person must be affected by ALS (Byrne et al,

2010). A more lenient definition states that at least one relative of the affected is affected by a motor neuron disease, which does not have to be ALS. The lack of information on family history, and incomplete penetrance of genes further complicate differentiation between the two types of ALS.

ALS is a multifactorial disease involving different cell types that contribute to the pathological mechanism. Nowadays mutations in 21 different genes have been linked to ALS (Al-Chalabi et al., 2012). It is not a pure motor neuron disease. These ALS-causative genes link ALS in development of a spectrum of other neurodegenerative diseases such as frontotemporal lobar degeneration (FTLD), and Parkinson's disease. For instance, a typical ALS case can occur with or without FTLD. There are physiological and neuropathological overlaps in these ALS-causative genes. Several of them share similar cell functions, such as RNA metabolism, and co-localize in intra-neuronal aggregates/inclusions.

1.1. SOD1

Although the disease was first documented and characterized by Jean-Marie Charcot in the 1870s, the first causative gene was not discovered until a century later (Rowland, 2001). In 1993, researchers identified copper/zinc superoxide dismutase 1 (SOD1) as the first causative ALS gene (Rosen et al., 1993). Since then 160 mutations in SOD1 have been identified (Gurney et al., 1994; Menzies et al., 2002). SOD1 is a ubiquitous homo-

dimer located in the glial cells and motor neurons of the spinal cord (Nagai et al., 2007; Pasinelli et al., 2006; Valdmanis et al., 2008). The main function of SOD1 is to protect cells from oxidative damage by metabolizing superoxide radicals (Gurney et al., 1994; Niwa et al., 2007). The SOD1 protein misfolds when mutated and these SOD1 mutations have been linked to ALS pathology through a number of different pathways such as mitochondrial dysfunction and oxidative stress (Bosco et al., 2010; Crow et al., 1997).

Researchers have investigated SOD1 mechanism underlying the disease by generating plethora of over 30 different animals' models and overexpressing human SOD1 *in vivo* and *in vitro*. These studies have led to the development of therapeutic strategies targeting specific pathways. Though some trials showed promised in rodent models, but they failed to perform in clinical human trials. The research on SOD1 contributed to understanding the pathological mechanism involved in motor degeneration in ALS, but the mutations in SOD1 gene only account for 10-20% of all familial ALS cases, 1% of sporadic ALS cases, and less than 2% of cases of ALS (Boillee et al., 2006). There is still a lack in the depth understanding of the other sporadic and familial ALS.

1.2. TDP-43

In 2006, the second major ALS causative gene was discovered. This discovery led to a major shift in understanding of ALS pathologies (Neumann et al., 2006). One of the notable ALS pathological manifestations is the ubiquitinated intraneuronal inclusion in dying motor neurons (Leigh et al., 1989). In 2006, a major component of the inclusion was identified as transactive response-DNA binding protein 43 kDa (TDP-43), encoded by the *TARDBP* gene. Shortly after, the ALS causing mutations in the gene was uncovered. It was reported to be a causative component of both familial and sporadic ALS. TDP-43 is a component of ubiquitinated neuronal inclusion in sporadic ALS and FTLD with ubiquitinated inclusions. These two diseases are part of one disease referred to as TDP-43 proteinopathy.

TDP-43 is a ubiquitously expressed protein among different tissues and with an elevated level during development. TDP-43 was originally identified as a transcriptional repressor that binds to human immunodeficiency virus type 1 TAR DNA sequence motifs (Ou et al., 1995). The protein is involved in RNA metabolism, and preferentially binds to RNAs with long introns especially those involved neuronal synaptic and developmental functions. Some of those proteins encoded by the RNA contribute to neurodegenerative disease (Polymenidou et al., 2011). More than 40 ALS causative *TARDBP* gene mutations incur in the glycine rich domain, which is crucial for protein-protein interaction (Gitcho et al., 2008; Kwiatkowski et al., 2009; Sreedharan et al., 2008).

TDP-43 is predominantly nuclear in the normal state, but mislocalized to the cytoplasm alongside stress granules in diseased states (Mackenzie et al., 2007; Neumann et al., 2006; Van Deerlin et al., 2008). The TDP-43 found in cytoplasmic aggregates are heavily modified by ubiquitination, phosphorylation, and misfolding. TDP-43 depletion affects the expression of splicing of many different RNAs. The loss of TDP43 has shown to be detrimental in knockout rodent models (Sephton et al., 2010; Wu et al., 2010; Chiang et al., 2010). However overexpression has also shown to be toxic (Joyce et al., 2011).

The identification of TDP-43 was soon followed by the discovery of an ALS causative gene, Fused in Sarcoma (FUS) protein, as the primary cause of ALS6 (Kwaitkowski et al, 2009; Vance et al., 2009).

1.3. FUS

Shortly after the discovery of TDP-43, the second RNA/DNA-binding ALS causative molecule, named FUS, was identified (Kwiarkowski et al., 2009; Vance et al., 2009). FUS has structural and functional similarities to TDP-43. Both wild types of TDP-43 and FUS are found in intraneuronal aggregates in Parkinson and Alzheimer's diseases (Lagier-Tourenne et al., 2009). Similar to TDP-43, FUS mutations are also found in some forms of FTLD. However, it has been observed in ALS that the accumulation of FUS and TDP-43 in intraneuronal cytoplasmic aggregates is mutually exclusive (Ling et al., 2010). While TDP-43 mutations account for 5% of familial ALS, FUS mutation is less frequently and

consists of 4% of familial ALS (Yokoseki et al., 2008; Vance et al., 2009). Despite the low frequencies of involvement, the discovery of these two RNA/DNA-binding proteins is considered a milestone in ALS research, because of the wide spread presence of these proteins in intraneuronal aggregates are characteristic of tissues samples from sporadic ALS.

1.3.1. Structure

FUS consists of 526 amino acid encoded by the 15 exons of FUS gene located on chromosome 16. Like TDp-43, it is ubiquitously expressed. FUS belongs to the FET protein family, which includes the Ewing sarcoma (EWS) protein (Kovar et al., 2011). The FET protein family typically localizes to the nucleus and is involved in RNA and DNA functions (Deng et al., 2014). The protein structure is characterized by an N-terminal domain enriched in serine, tyrosine, glycine, and glutamine, a glycine rich region, an RNA recognition motif, followed by two regions rich in arginine/glycine/glycine repeats separated by a zinc finger motif, and a highly conserved nuclear localization signal (NLS) sequence **Figure 1**. The N-terminal end contains domains involved in transcriptional activation. The C-terminal end is involved in RNA binding.

Figure 1. Structure of FUS

FUS has an N-terminal region rich in serine, tyrosine, glycine, and glutamine, a glycine-rich region, an RNA recognition motif, two regions rich in arginine/glycine/glycine repeats separated by a zinc finger motif. At the C-terminal, it has a highly conserved nuclear localization signal.


N
SGYQ-rich
Gly-rich
RRM
RGG-ZnF-RGG
PY-NLS
C

1.3.2. Function

FUS was originally identified as a sarcoma gene. Its involvement in gene arrangements has been implicated in myxoid liposarcoma and low grade fibromyxoid sarcoma. FUS is an RNA/DNA binding protein that is involved in multiple levels of RNA metabolism; such as, transcription, splicing and interacts with a wide array of proteins. The protein is mainly located in the nucleus, but shuttles between the nucleus and the cytoplasm.

FUS has important roles in each of the two compartments. In the nucleus, FUS regulates critical steps of RNA metabolism. In particular: transcription, nuclear-cytoplasmic mRNA transport, alternative splicing of pre-mRNA, and processing RNA containing long-introns. FUS self regulates and maintains protein homeostasis through alternative splicing. Many of these molecules targeted by FUS are associated with neurogenesis, gene expression regulation, and DNA damage response. Recent research suggests nuclear FUS is essential for neurogenesis, the growth and development of the neuron. A disruption of FUS RNA metabolism results in the lack of DNA repair and contributes to genomic instability. In the cytoplasm, FUS accompanies mRNA transportation to specific sites in the dendritic spines of the neuron for localized or site-specific protein translation, which contributes to the morphology and function of the spines, such as in synaptic functions (Zhou et al., 2014).

1.3.3. Mutation

While in healthy patients, FUS is predominantly localized to the nucleus; in ALS patients FUS is trapped in cytoplasmic inclusions, which hinders it from transporting mRNA to the spines. FUS cytoplasmic inclusion is characteristic pathology of neurons and glial cells in ALS6 (Zhou et al., 2014). The lack of site-specific protein translocation contributes to the changes in neuron morphology and function. The cytoplasmic inclusion of FUS is accompanied by a decrease in the level of nuclear FUS. The decreased FUS protein level and altered function of FUS in the nucleus render FUS defective in metabolizing RNA involved in DNA damage response pathway, gene expression regulation. The lack of FUS-modulated DNA repair leaves the cells more vulnerable to stress and mutation. It in turn promotes neurodegeneration, as observed in the progressive degeneration of upper and lower motor neurons in ALS. Unlike TDP-43 knockouts, FUS knockout in different mouse strains obtained different outcome, which suggested the genetic background of the mice, play a possible role as modifiers. The overexpression of FUS mutant in mouse models has displayed ALS and FTLD-like pathologies, and overexpression of wild-type FUS resulted in progressive motor neuron degeneration in a dosage-dependent fashion (Mitchell et al., 2013).

The exact meaning behind mislocalization of FUS in ALS and other neurodegenerative disease is still debated. There are proposed theories but it is still unclear whether the intraneuronal inclusions actively participated in the course of the disease or are simple end products of deregulated cell metabolism. In 2010, Dormann et al. proposed a two-

hit model of FUS ALS pathology. In the first hit, there is a nuclear import defect, where the ALS-associated FUS mutation hinders interaction with Trn1 and subsequently results in the accumulation of FUS in the nucleus (Dormann et al., 2010). In the second hit, the mutant FUS retained in the cytoplasm is recruited into stress granules. The persistence of cellular stress leads to the prominent pathological inclusions observed in FUS-associated ALS. In post-mortem analysis of the brains and spinal cords of ALS6 patients, the degree of cytoplasmic FUS aggregation and granule formation is directly correlated with age of disease onset.

To date, up to 50 ALS causative mutations in the FUS gene have been identified. Dominant missense point mutation is the most common, and others being insertion, deletion, and truncation. These mutations are mostly autosomal dominant in familial ALS (Kwiatkowski et al., 2009; Vance et al., 2009; Van Langenhove et al., 2010). Unlike the mutated sites in TDP-43, which are at the glycine-rich regions, majority of the FUS mutations are located at the highly conserved C-terminus containing the non-classical proline-tyrosine nuclear localization signal (Mackenzie et al., 2010).

Both TDP-43 and FUS are involved in RNA metabolism, and it has been suggested that there might be a common disease mechanism underlying sporadic and familial. An in depth understanding of FUS pathology may also provide insight into the mechanism ALS causative gene and provide a deeper understanding of ALS and allows the possibility of a common therapeutic strategy to benefit a broad spectrum of patients. My thesis focuses on identifying kinases affect the subcellular localization of FUS through post-

translational modification.

1.3.4. Non-classical PY-NLS

FUS has a non-classical proline-tyrosine nuclear localization signal (PY-NLS). This disordered and positively charged signal contains a central basic motif followed by a C-term consensus sequence containing PY.

Trn1, a subunit of the karyopherin receptor complex, recognizes the PY-NLS consensus sequence and imports FUS into the nucleus. Nuclear import of FUS is dependent on transportin 1 (Trn1) (Fujii et al., 2005). Previous studies have shown the terminal tyrosine on FUS is for Trn1 interaction and nuclear transportation (Lee et al. 2006, Fujii et al., 2005). In a study comparing the binding affinity between wild type FUS NLS and ALS-causative FUS NLS with Trn1 showed that when the terminal tyrosine was mutated to an aspartic acid (Y526A), the binding affinity with Trn1 was reduced by approximately 500 times and accompanied by an increased amount of FUS mislocalized to the cytoplasm (Niu et al., 2012).

Phosphorylation of tyrosine residues in NLS in proteins often induces critical structural changes for function/recognition, and most importantly subcellular localization. Sam68 and EWS are two proteins homologous to FUS **Figure 2**. The phosphorylation of their tyrosine residues is critical to their nuclear localization.

Figure 2. Nuclear localization sequence alignment for Sam68, EWS, and FUS.

The corresponding amino acids in the nuclear localization sequences are highlighted in yellow. Y435, Y440, Y443 of Sam68 are phosphorylated by Brk. Phosphorylation of Y440 is critical to the nuclear localization of Sam68 and corresponds to Y656 of EWS. Similarly, the phosphorylation of Y656 of EWS is critical to EWS nuclear import. In turn, Y656 of EWS corresponds to Y526 in FUS.

Sam68	420 RPSLKAPPARPVKGAYREHPYGRY 443
EWS	639 PGKMDKGEHRQERRDRPY 656
FUS	495 RGGRGGGDRGGFGPGKMDSRGEHRQDRRERPY 526

Sam68 is a c-Src-associated substrate during mitosis of 68 kDa. The C-terminal region harbors an NLS comprised of the last 24 amino acids of the protein (Ishidate et al., 1997). Brk, a growth-promoting non-receptor tyrosine kinase phosphorylates the three tyrosines (Y435, Y440, Y443) in the NLS. The phosphorylation of Y440 has been demonstrated to be the principle modulator that dictates the nuclear localization of the protein (Ishidate et al., 1997; Lukong et al., 2005). Phospho-mimetic substitution of Y440F disrupts Sam68's importation process and causes it to mislocalize to the cytoplasm, while mutating the other two tyrosines had no effect on the nuclear localization of the protein (Lukong et al., 2005).

Sam68 is highly homologous to EWS as they are both BTK-SH3 binding proteins. Y440 on Sam68 corresponds to Y656 of EWS. Similar to FUS, the nuclear import of EWS is mediated by Trn1. When phosphorylation on the PY-NLS tyrosine, Y656, is abolished, EWS accumulates in the cytosol and co-localize with Trn1. Aspartic acid and phenylalanine substitution cannot restore the nuclear localization of the protein (Leemann-Zakaryan et al., 2001). Thus the terminal Y is very important to EWS localization.

Furthermore, EWS and FUS are both members of the FET protein family, and Trn1 mediates their nuclear import (Lee et al., 2006).

Modification of proteins by phosphorylation is critical mechanism to control the function and structure of a protein as well as its pathways. As mentioned above, phosphomimetic substitution of Y526 results in the cytoplasmic mislocalization and

cytosol accumulation of FUS. Previous studies showed Y526 on PY-NLS of FUS is crucial to the nuclear localization of FUS. The corresponding tyrosine in SAM68 and EWS are phosphorylated for proper nuclear localization and function. The phosphorylation of tyrosine residues in NLS of Sam68 and EWS strongly suggests the phosphorylation of tyrosine residues in the FUS-NLS is critical to its interaction with Trn1 and subcellular localization. Y656 of EWS corresponds to the terminal tyrosine, Y526 on PY-NLS of FUS. There are up to 19 phosphorylation sites identified on FUS. Majority of the sites are located at the RNA-recognition motif, and two at the C-terminus, S462, and Y468. A detailed description of the location can be found at PhosphoSitePlus®, www.phosphosite.org **Figure 3** (Hornbeck et al., 2012).

Figure 3.Sites of phosphorylation on FUS

Majority of the phosphorylation sites are found in the RNA-recognition motif. Phosphorylation sites, S462, and Y468, are at the C-terminus, S462, and Y468.

Adapted from PhosphoSitePlus®, www.phosphosite.org. Copyright permission not required as content is in the public domain.

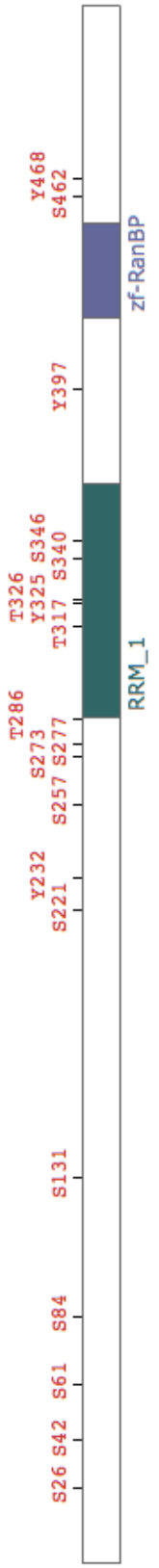
Y468
S462
zf-RanBP
Y397
T326
Y325
S346
S340
T317
RRM_1
T286
S273
S277
S257
Y232
S221
S131
S84
S61
S42
S26

Since majority of the ALS causative mutations in FUS are located at the C-terminus, the post-translational modification of the C-terminus is of particular interest to us. The post-translational modification of amino acids in the C-terminal sequences as shown in Sam68 and EWS suggest that the post-translational modification of FUS at the similar region could be crucial to the localization of FUS.

1.4. Hypothesis and Aims

We hypothesize that the post-translational modification of FUS amino acids at the C-terminus is crucial to its subcellular localization and function.

The aim of our study is to conduct a kinome-wide RNA interference (RNAi) screen to identify kinases that post-translationally modify FUS and affecting its subcellular localization.

We chose high content RNAi analysis with automated microscopy because this method has low false positives and high sensitivity. It permits the analysis of individual cells at a subcellular level, which is crucial for studying the mislocalization of FUS from the nucleus to the cytoplasm. Since not much is known about the post-translational modification of FUS and the modulators involved in the function of FUS, the screen can provide a significant of amount of data. The disadvantage to conducting a high content screen is the amount of time and effort distributed to develop, optimize complex assays, and adjusting automated image analysis systems for the particular experiment.

Chapter 2: Materials and Methods

2.1 Cell Culture

Cells were grown in Dulbecco's Modified Eagle's Medium (Sigma) supplemented with 10% fetal bovine serum (Life Technologies) in humidified 10% CO2 incubator at 37°C. 1% (w/v) of penicillin and streptomycin were added to the medium for the RNAi kinome screen. Human osteosarcoma cell line (U2OS), HeLa, Human ovarian carcinoma cell line (SKOV3), and human primary glioblastoma cell line (U87MG) were used in the study. U2OS, HeLa and SKOV3 cells were kindly provided by Professor R. Screaton (Department of Biochemistry, Microbiology and Immunology, University of Ottawa, Ottawa, Canada).

2.2 Transfection

Transfection in 6-well plates and 4-chamber slides was performed as outlined in *Thermo Scientific DharmaFECT Transfection Reagents – siRNA Transfection Protocol* manual (Thermo Scientific).

In 384-well plates, cells were transfected using reverse transfection protocol, where 5 µL of 50 nM siRNAs and equal volume of 0.05 RNAi MAX (Life Technologies) were plated to form transfection complexes prior to the addition of 600 cells in 30 µL of cell media. 40 µL of cell media was added to the surrounding wells to prevent evaporation. The plates were then incubated at 37°C for 72 hours prior to analysis.

2.3 Immunofluorescence staining

Immunofluorescence staining was performed in 4-chamber slides and 384-well plates using different protocols.

2.3.1. Immunofluorescence staining in 4-Chamber slide

Immunofluorescence (IF) staining in 4-chamber slides was performed manually. Slides were briefly rinsed with phosphate-buffered saline pH7.4 (PBS) and fixed in 4% paraformaldehyde for 20 minutes. After washing in three changes of PBS, blocking was performed by incubating cells with 5% normal goat serum (Santa Cruz Biotechnologies) for 30 minutes. Primary antibodies were diluted in blocking solution as listed in **Table 1** and incubated overnight at 4**°**C. Slides were again washed with three changes of PBS and the incubated with secondary antibodies as listed in **Table 1** for 40 minutes in the dark. Following another set of PBS washes, slides were mounted using VECTASHIELD HardSet Mounting Medium with DAPI (#H-1500, Vector Laboratories) and sealed with nail polish to prevent cover from shifting when used under the microscope.

Table 1. Primary and secondary antibody information

Antigen	Source	IF Dilution	Western Dilution
FUS	Milipore Mouse monoclonal #04-1552	1:1000	1:500
CLK1	Santa Cruz Goat polyclonal #sc-47957		1:200
Phosphotyrosine	Cell Signaling Mouse monoclonal #9411	-	1:2000
Phosphoserine	Milipore Rabbit polyclonal #AB1603	-	1:500
Goat anti-Mouse IgG Alexa Fluor 594	Invitrogen #A-11032	1:1000	-
Goat anti-Mouse IgG Alexa Fluor 488	Invitrogen #A-11001	1:1000	-
X anti mouse		-	1:5000
Rabbit anti-goat		-	1:5000
Anti-rabbit		-	1:5000

2.3.2. Immunofluorescence staining 384-well plate

Immunofluorescence staining in BD Falcon 384 well plates utilized a multi-drop reagent dispenser (Thermo Scientific) to add reagents to the wells, and HTS Biotek Elx405 CW select plate washer (Biotek) for washes and aspirations. Cells were fixed with 1.85% formaldehyde and 1 µg/mL Hoechst (Life Technologies) in cell culture medium for 15 minutes at 37°C. Glycine/PBS solution was then added and incubated for 4 minutes to inactivate the remaining formaldehyde. Next cells were incubated with 30 µL of 0.1% Triton X-100/PBS for 2 minutes before blocked with 3% bovine serum albumin (BSA) in PBS for 1 hour. Primary antibodies diluted in 3% BSA/PBS as listed in **Table 1** and incubated overnight at 4°C. After a wash cycle with final aspirate, secondary antibodies were diluted 3% BSA/PBS as listed in **Table 1** and incubated for 45 minutes. After three washes, clear plate seals were added and ready for imaging.

2.4 Lysate collection

U87MG cells were washed with PBS and lysed in a cold lysis buffer consisted of Frack's buffer, 1x Roche Complete Protease Inhibitor Cocktail Tablets (Hoffmann-La Roche), 2 mM NAF, 2mM NaPPi, 2 mM $NaVO_4$, and 2mM PMSF. Then cells were scraped off the plate, collected into an Eppendorf tube, and sonicated three times for 10 seconds each, and spun down at 4 000 rpm for 20 minutes at 4°C. The supernatant was then transferred to a new tube for further analysis or stored at -80°C.

2.5 RNAi kinome screen

QIAGEN human kinome siRNA library (Qiagen) targeting over 700 kinases was used in this study. The library was divided into three sets and the screen was performed in triplicates with a total of nine assay plates. Reverse transfection and IF staining in 384-well plates were performed as described above. Dr. Stephen Baird (Manager, High Throughput Screening Lab, CHEO Research Institute) optimized the imaging algorithm and scanned the plates using Opera High Content Screening system (PerkinElmer). Columbus (PerkinElmer Inc.), data analysis software, was used to quantify the intensity/amount of FUS in the nuclei and cytoplasm. The quality of the kinome screen was assessed by calculation Z-prime factor. Kinases with statistically lower nucleus to cytoplasmic FUS intensity ratio than the negative control were potential hits and were pursued for further analysis.

The sequence of the convoluted siRNAs from Qiagen targeting CLK1 can be found in **Table 2**.

Table 2. Sequence of siRNAs targeting CLK1.

siRNA	Sequence
CLK1_1	CACGATAGTAAGGAGCATTTA
CLk1_2	AACGTGATGAACGCACCTTAA
CLK1_5	AAAGCCGGTATCAGAACCATA
CLK1_6	GAGAAAGATTATCATAGTCGA

2.6 Immunoprecipitation

400 µg of protein lysate diluted in lysis buffer, 2 µL of antibody targeting the protein of interest and 20 µL of nProtein A Sepharose beads Fast Flow (GE Healthcare Life Sciences) were combined in an Eppendorf tube. After rotating the tube in the cold room overnight, the beads were spun down and washed with NETN lysis buffer three times. Next 20 µL of PBS and 8 µL of sodium dodecyl sulfate dye were added, and boiled at 95°C for 5 minutes. The beads are spun down and analyzed using Western blotting.

2.7 Western blotting

The blot was blocked with 5% non-fat milk in Tris buffered saline with Tween® 20 (TBST) for 30 minutes at room temperature. Primary antibodies were diluted with 5% non-fat milk as listed in **Table 1** and incubated for 1 hour at room temperature or at 4°C overnight. The blot was rinsed with TBST before adding secondary antibodies diluted in 5% non-fat milk as listed in **Table 1**.

2.8 *In vitro* kinase assay

Khalid Al-Zahrani from Sabourin Lab (Department of Cellular and Molecular Medicine, Faculty of Medicine, University of Ottawa) kindly performed the *in vitro* kinase assay experiments.

Chapter 3: Results

3.1 Cell line selection

It was essential to find a suitable cell lines to study the mislocalization of FUS. The cell line must express an adequate level of FUS and a flat cell morphology that is suitable for visualizing FUS translocation between the nucleus and cytoplasm using IF staining under the microscope. Data collected through Genecards.org revealed high endogenous FUS protein expression in nervous, musculoskeletal, and reproductive cell lines (Higdon et al., 2013; Stelzer et al., 2012; Schaab et al, 2012; Wang et al., 2012). Based on the data and the cell lines available at the laboratory, we selected U2OS, HeLa, SKOV3, and U87MG, and immunofluorescence stained for FUS in 384-well plate to test their ability to be used for the screen.

U87MG showed the strongest FUS staining in the nucleus, followed by SKOV3, HeLa, and U2OS **Figure 4**. U87MG has a flat morphology, a distinct nucleus with a large cytoplasm, making the cell line suitable for visualizing the mislocalization of FUS from the nucleus to the cytoplasm. Hence, we chose to use U87MG in the kinome screen because of its strong FUS staining and its flat morphology.

Figure 4. Immunofluorescence staining of FUS in U2OS, HeLa, SKOV3 and U87MG.

FUS was stained with primary antibody at 1:1000 dilution (in green). Nucleus was stained with Hoechst (in blue).

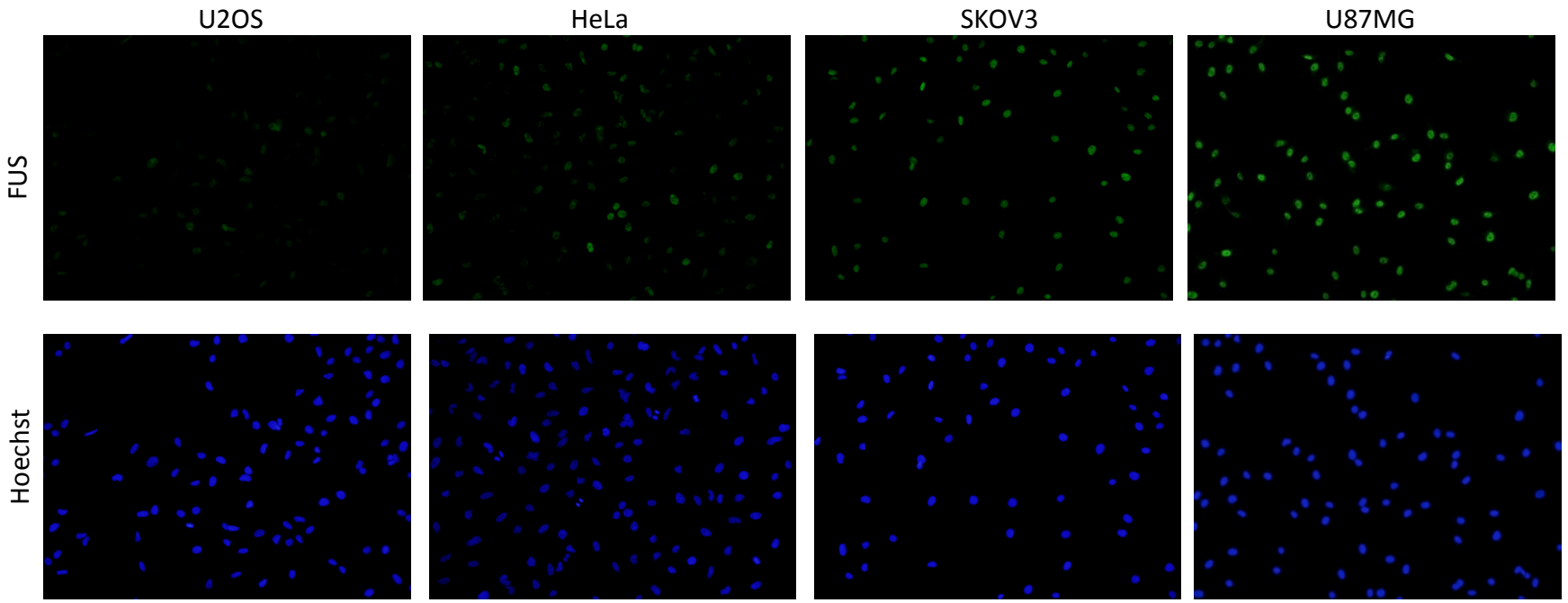
U2OS
HeLa
SKOV3
U87MG
FUS
Hoechst

3.2 Antibody Specificity

Prior to optimizing U87MG cell to be used in the kinome screen, it was crucial to validate the specificity of the FUS antibody (Milipore Mouse monoclonal #04-1552) and its corresponding secondary antibody to eliminate the possibility of a cross-reaction with other proteins.

To determine the specificity of the primary antibody, IF and western were performed using U87MG cells transfected with either non-specific siRNA (negative control) or FUS siRNA. The cells were stained for FUS in both experiments. In IF, no green fluorescence staining for FUS was observed in cells transfected with FUS siRNA **Figure 5**. On the western blot, there was a significant reduction in FUS in the cells transfected with FUS siRNA in comparison to the negative control **Figure 6**. The lack of FUS staining in cells transfected with FUS siRNA confirms the specificity of the primary antibody.

Furthermore, to ascertain the specificity of Goat anti-Mouse IgG Alexa Fluor 488 (Invitrogen #A-1101) against the primary antibody, immunofluorescence staining in U87MG cells was performed in the presence and the absence of the primary antibody **Figure 7**. No FUS staining was observed in the absence of the primary antibody which suggests the secondary antibody does not cross interact with other proteins in the cell.

Figure 5. Immunofluorescence staining of FUS in U87MG cells transfected with non-specific or FUS siRNA.

FUS was stained with primary antibody at 1:1000 dilution (in green). Nucleus was stained with Hoechst staining (in blue). The overlap images of the FUS and Hoechst staining show the absence of FUS staining in U87MG transfected with FUS siRNA.

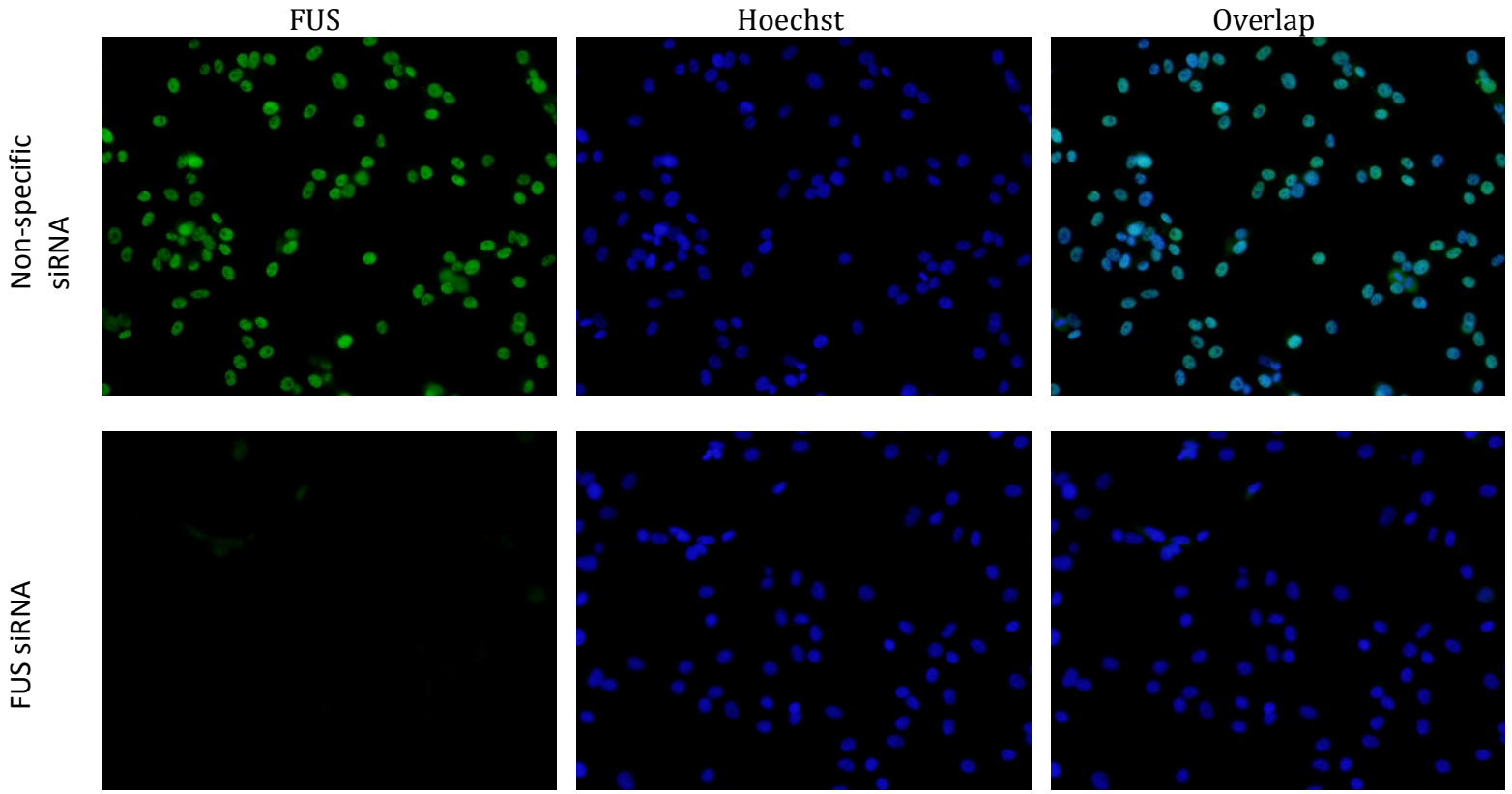
FUS
Hoechst
Overlap
Non-specific siRNA
FUS siRNA

Figure 6. Western blot staining for FUS in U87MG cells transfected with non-specific or FUS siRNA.

FUS was stained with primary antibody diluted at 1:500. There is a significant reduction in the amount of FUS in U87MG cells transfected with FUS siRNA in comparison to the cells transfected with non-specific siRNA.

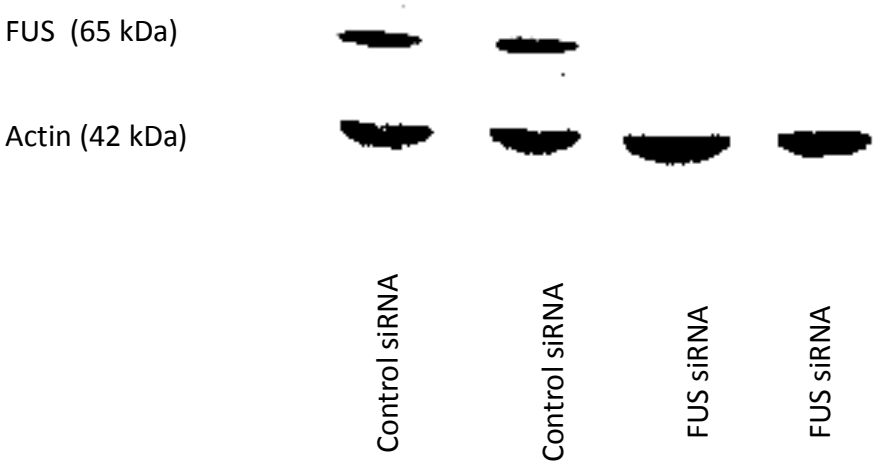
FUS (65 kDa)
Actin (42 kDa)
Control siRNA
Control siRNA
FUS siRNA
FUS siRNA

Figure 7. Immunofluorescence staining of FUS in U87MG cells with or without primary antibody.

FUS was stained with primary antibody at 1:1000 dilution (in green). Nucleus was stained with Hoechst (in blue).

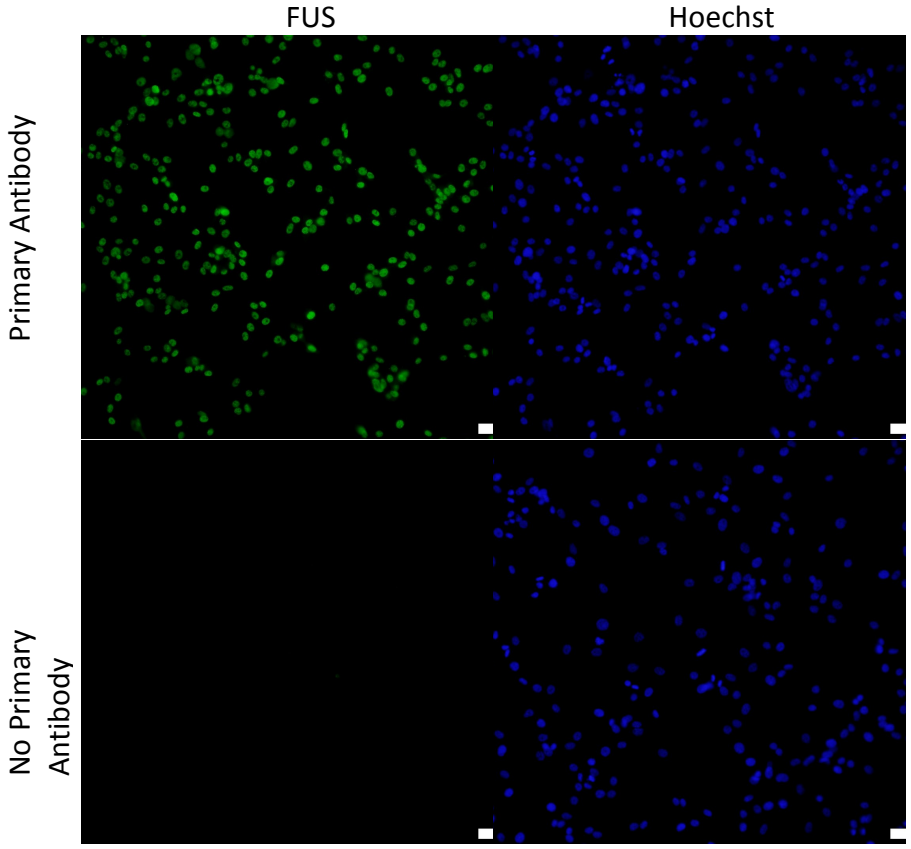
FUS
Hoechst
Primary Antibody
No Primary Antibody

3.3 Kinome Screen Optimization

A number of different parameters such as transfection protocol, immunofluorescence staining protocol, imaging and detection algorithms were optimized to achieve strong signal to background ratio and low variations between the wells. The statistical significance between the negative and the positive controls was determined using the Z prime factor. U87MG cells transfected with non-specific siRNA were used the negative control, and cells transfected with transportin 1 and 2 siRNAs (Trn) were used as positive controls **Figure 8**. Two transportin siRNAs as oppose to just one was used to prevent cross-reactions. The Z-prime factor between the positive and the negative controls was 0.7 which falls between the optimal range of 0.5 and 1.0, indicating a statistical significance between the positive and negative controls in this study.

An alternative positive control using M9M peptide inhibitors was created to assist in calibrating FUS mislocalization in the screen. The goal was to achieve a higher statistical significance, in other words, a higher Z-prime factor value. However, M9M peptide inhibitor was toxic to the cells and resulted in significant cell death. Hence it was not utilized as positive control. Further information for M9M peptide inhibitor can be found in the appendix.

Figure 8. Formula for Z-prime factor calculation

The Z-prime factor measures the statistical significance of the positive and the negative controls for high throughput assays. It is based on four parameters, the means, μ, and standard deviations, σ, of the positive, p, and negative, n, controls. A value between 0.5 and 1.0 indicates statistical significance between the positive and negative controls. The positive and negative controls are the nucleus to cytoplasmic FUs intensity ratio of U87MG cells transfected with transportin 1 and 2 siRNAs (Trn) (1.70 ± 0.07) and non-specific siRNA(7.61 ± 0.51) respectively. The Z-prime factor from the screen was 0.70039031.

$$Z - prime\ factor = 1 - \frac{3(\sigma_p + \sigma_n)}{|\mu_p - \mu_n|}$$

3.4 Kinome Screen Analysis

Data from the screen uploaded to Columbus (PerkinElmer Inc.) was used to analyze each kinase and identify potential positive hits. Several parameters, such as cell number, cytoplasmic and nucleus FUS intensities were examined and compared to the controls.

First, wells with a significant reduction in cell number were disregarded because the kinases knocked down were most likely crucial to the cell's viability. Second, the average and standard deviation nucleus to cytoplasmic FUS intensity ratio were calculated for each hit with the outliers excluded. The hits with values within the standard deviations of the negative controls were removed. A low ratio of nucleus to cytoplasmic FUS intensity implies a decrease in amount of nuclear FUS relative to the cytoplasmic value, or an increase in cytoplasmic FUS relative to the nucleus. It is vice versa for a high ratio. The kinases with values in the range of the negative control (7.61 ± 0.51) were eliminated because they are not stastical significant **Figure 9.** Nuclear and cytoplasmic values were also considered individually for the remaining kinases. A list of potential hits is shown in **Table 3.** Lastly, we examined the images and the function of these remaining kinases to further eliminate false positives. Among the potential hits, we decided to pursue validating CLK1 **Figure 10**.

Figure 9. Distribution of data from RNAi kinome screen based on nucleus to cytoplasmic FUS ratio.

The negative and positive controls are shown as red square and green triangles respectively. Majority of the hits are within the range of the negative control. The hits within the range of the negative controls were eliminated.

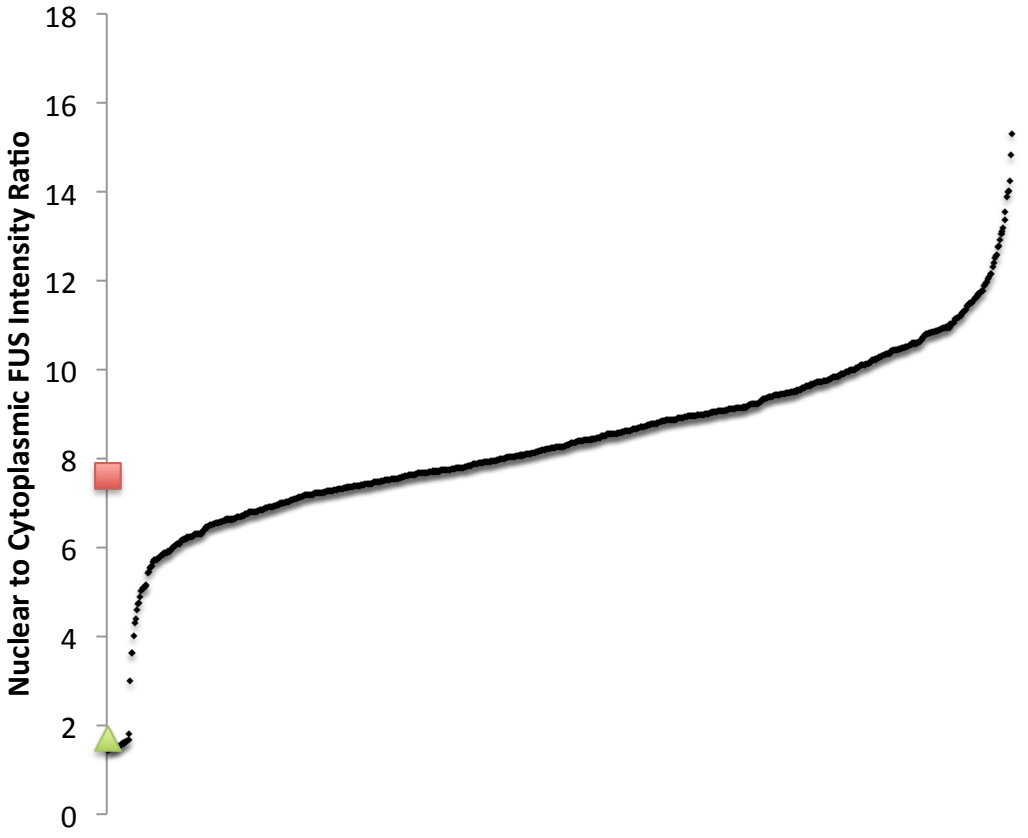
Nuclear to Cytoplasmic FUS Intensity Ratio
18
16
14
12
10
8
6
4
2
0

Table 3. List of potential hits with corresponding FUS intensity value

Kinase		Nuclear FUS Intensity	Cytoplasmic FUS Intensity	Nuclear to Cytoplasmic FUS Intensity Ratio
NTRK2	Neurotrophic tyrosine kinase receptor, type 2	78.9742	15.0511	5.16207
PHKA2	Phosphorylase kinase, alpha 2 (liver)	54.7271	18.1962	3.00761
CSNK1G3	Casein kinase 1, gamma 3	106.885	17.4502	5.73385
GRK4	G protein-coupled receptor kinase 4	81.2397	18.5275	4.58596
CLK1	CDC-like kinase 1	107.283	18.6067	5.83875
BRAF	v-raf murine sarcoma viral oncogene homolog B1	116.041	18.7417	5.87896
RPS6KA4	Ribosomal protein S6 kinase, 90kDa, polypeptide 4	134.396	22.6588	5.7998
DGKE	Diacylglycerol kinase, epsilon 64kDa	141.397	26.1181	5.55886
NEK4	NIMA-related kinase 4	131.924	20.346	5.88002
TNK2	Tyrosine kinase, non-receptor, 2	113.567	19.6715	5.58304
DYRK3	Dual-specificity tyrosine-(Y)-phosphorylation regulated kinase 3	97.2138	16.3466	5.71878
ZAP70	Zeta-chain (TCR) associated protein kinase 70kDa	83.8407	14.3575	5.83952
HUNK	Hormonally up-regulated Neu-associated kinase	84.568	15.4338	5.7614
Negative Control		103.7639873	13.34815238	7.614508413
Positive Control		71.31279365	41.90298889	1.701143175

Figure 10. Immunofluorescence images of U87MG cells transfected with CLK1 siRNA from RNAi kinome screen stained for FUS

FUS is shown in green, and the nucleus is shown in red.

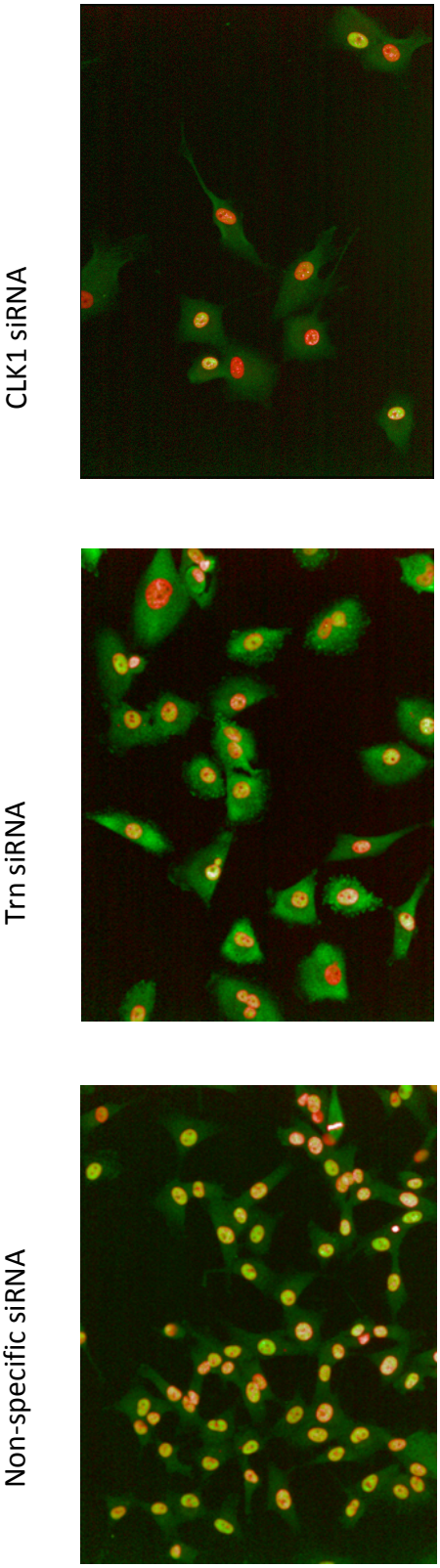
CLK1 siRNA
Trn siRNA
Non-specific siRNA

3.5 CLK1

CLK1 knock down cells had a nucleus to cytoplasmic FUS intensity ratio of 5.84. There was a greater increase in cytoplasmic FUS intensity (18.60) than in the nucleus (107.28) in comparison to the negative control with FUS intensities of 13.25 and 103.76 in the nucleus and cytoplasm respectively. The result was an overall decreased nucleus to cytoplasmic ratio similar to the positive control.

Furthermore when the number of cells is compared to the nucleus intensity of FUS, cells transfected with nonspecific siRNA shows majority of the cells are distributed in the centre of the graph **Figure 11**. The distribution of nucleus intensity in cells transfected with CLK1 siRNAs displays a left leaning pattern similar to the cells transfected with Trn siRNAs. The pattern shows that the distribution of nuclear FUS intensity in cells transfected with CLK1 is more similar to the positive control than to the negative control.

Figure 11. FUS nucleus intensity distribution in U87MG cells transfected with CLK1 siRNA.

The transfected cells are categorized in accordance to its FUS nuclear intensity number. The cells transfected with non-specific siRNA shows a central distribution, whereas the Trn and CLK1 siRNAs exhibit a similar left-leaning distribution.

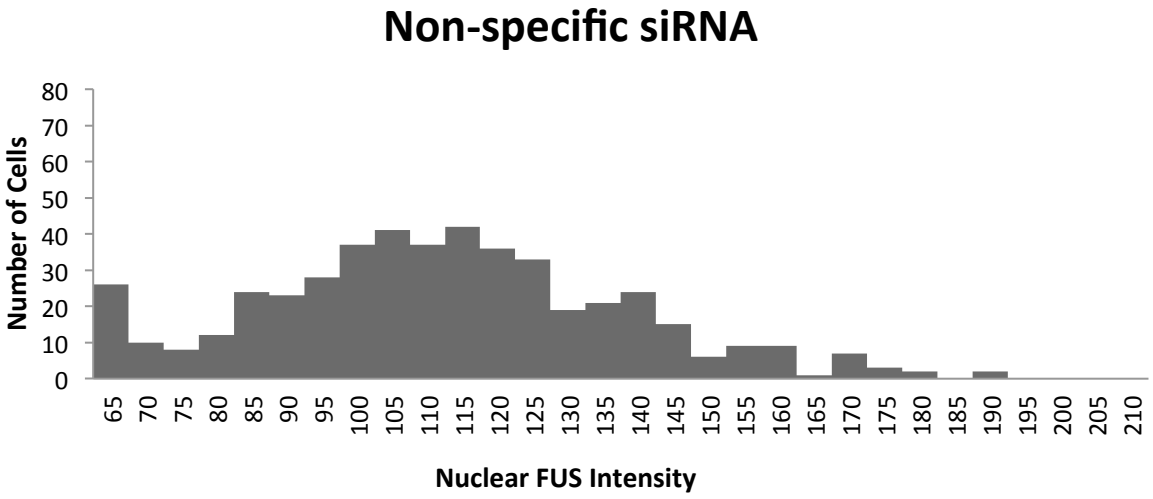
Non-specific siRNA
Number of Cells
0
10
20
30
40
50
60
70
80
65 70 75 80 85 90 95 100 105 110 115 120 125 130 135 140 145 150 155 160 165 170 175 180 185 190 195 200 205 210
Nuclear FUS Intensity

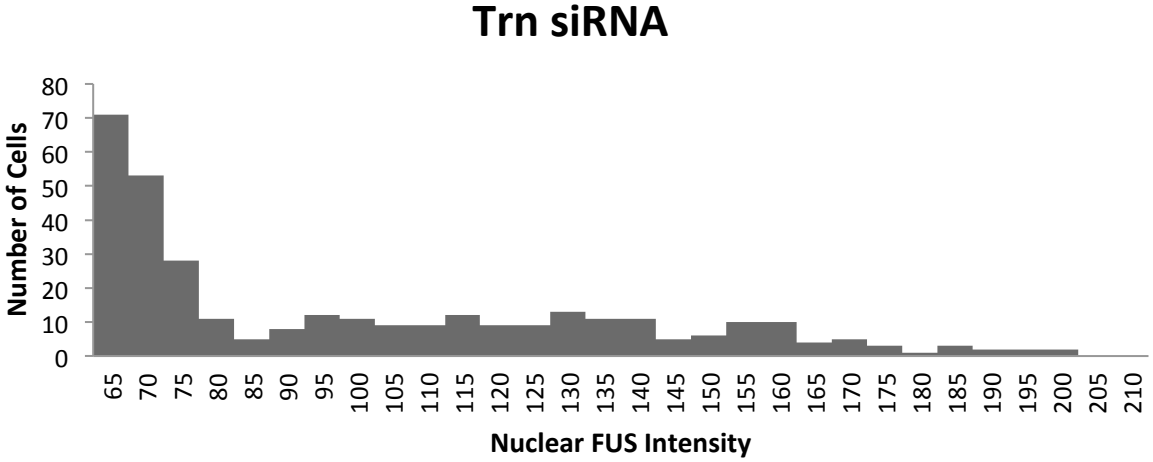
Trn siRNA
Number of Cells
0
10
20
30
40
50
60
70
80
65 70 75 80 85 90 95 100 105 110 115 120 125 130 135 140 145 150 155 160 165 170 175 180 185 190 195 200 205 210
Nuclear FUS Intensity

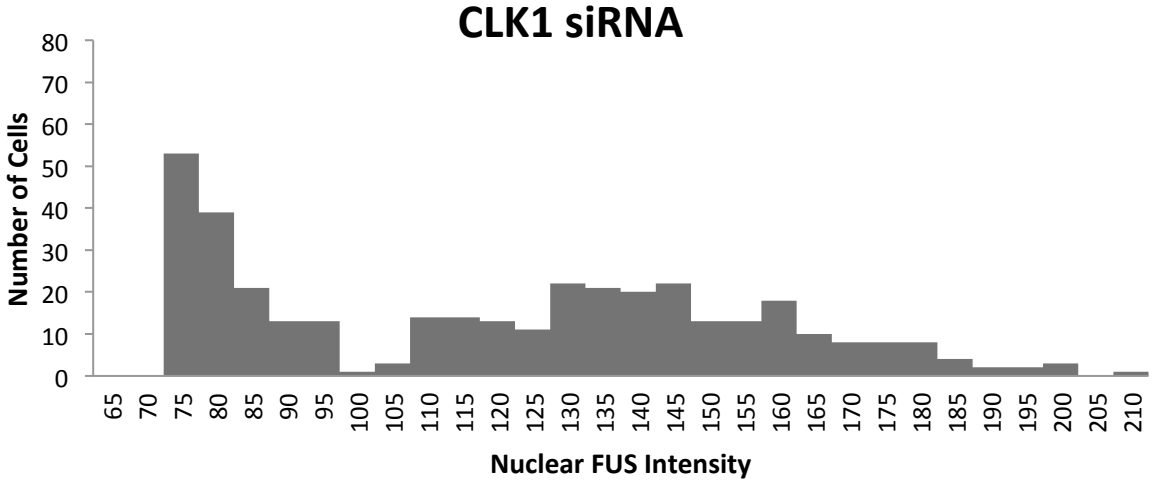
CLK1 siRNA
Number of Cells
0
10
20
30
40
50
60
70
80
65 70 75 80 85 90 95 100 105 110 115 120 125 130 135 140 145 150 155 160 165 170 175 180 185 190 195 200 205 210
Nuclear FUS Intensity

3.5.1. Deconvolution, drug inhibitor, and mutagenesis

CLK1_1, CLK1_2, CLK1_5, CLK1_6 are CLK1 siRNAs (GeneSolution siRNA Cat. No. 1027416), each targeting a different portion of the CLK1 siRNA and used together in the kinome screen In order to eliminate false positives, the siRNAs were deconvoluted and examined individually for the effect on FUS mislocalization.

U87MG cells were transfected with each individual CLK1 siRNA and IF stained for FUS **Figure 12**. Both CLK1_1 and CLK1_5 showed a decrease in FUS nuclear-to-cytoplasmic intensity ratio, with the latter being a more significant decrease. In contrast, CLK1_2 demonstrated a higher ratio, but an insignificant change in cells transfected with CLK1_6.

Western blot was used to determine the effect of CLK1_1, CLK1_2, and CLK1_5 on the level of FUS expression in the cells **Figure 13**. CLK1_6 was not tested because it showed insignificant change in the FUS ratio from the IF. The amount of FUS and actin levels were quantified. The ratio of FUS to actin was used to measure the change in FUS quantity. CLK1_1 and CLK1_5 showed a significant decrease in FUS level, while CLK1_2 had a less significant reduction on the amount of FUS.

Each of the CLK1 siRNAs appears to have a slightly different effect on the degree of FUS translocation and availability.

A drug inhibitor, TG 003, against CLK1 was also tested as an alternative to knock down CLK1 in U87MG cells. However, the results could not be repeated. Furthermore, mutagenesis experiment for CLK1_2 was attempted unsuccessfully. The targeted region has a high GC content that required a higher melting temperature for the primers than was permissible by the procedure.

Figure 12. Nuclear to cytoplasmic FUS intensity ratio for U87MG cells transfected with deconvoluted CLK1 siRNA and IF stained for FUS.

CLK1_1 and CLK1_5 transfected cells exhibit decrease in ratio. CLK1_2 siRNA increase the ratio, and no significant change in ratio was observed with CLK1_6 siRNA.

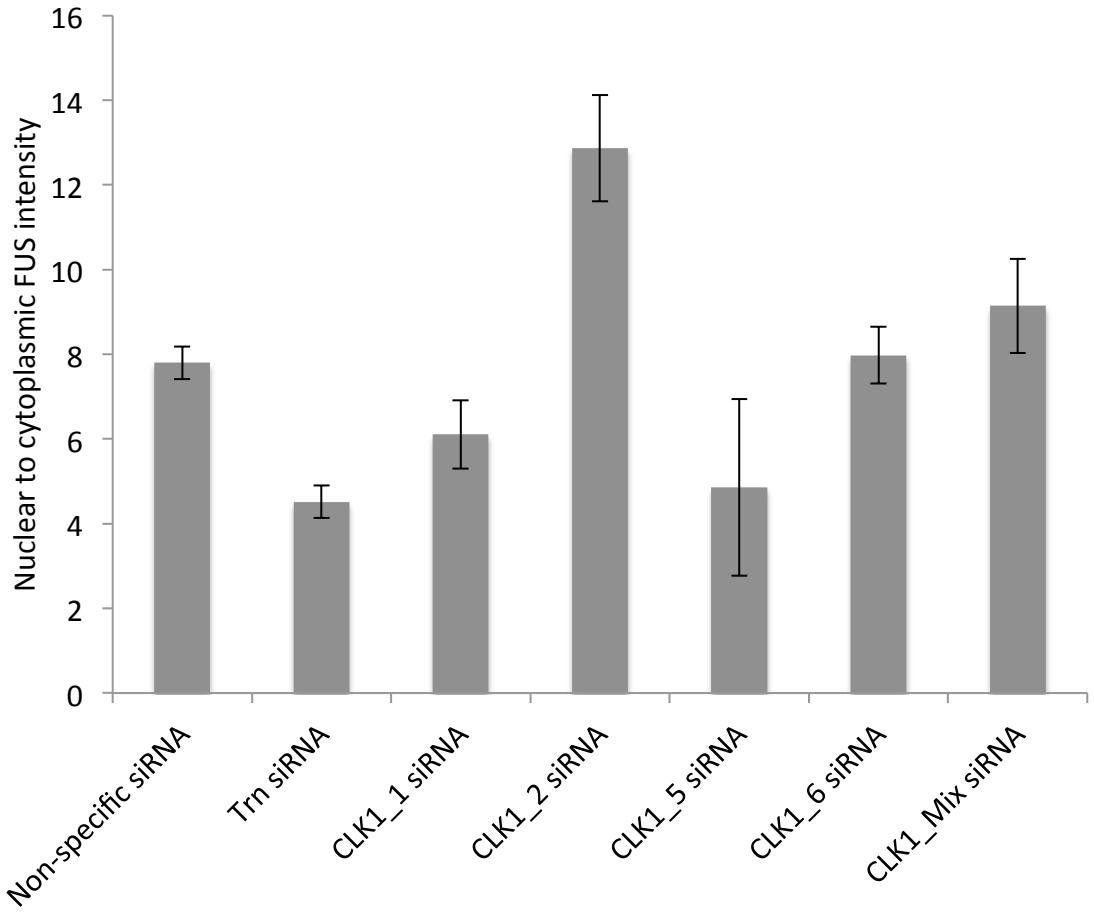
Nuclear to cytoplasmic FUS intensity
16
14
12
10
8
6
4
2
0
Non-specific siRNA
Trn siRNA
CLK1_1 siRNA
CLK1_2 siRNA
CLK1_5 siRNA
CLK1_6 siRNA
CLK1_Mix siRNA

Figure 13. FUS quantification in U87MG cells after transfection with different CLK1 siRNAs.

FUS and actin were quantified from the Western Blot. A ratio of FUS to actin was calculated to compare the changes in FUS in U87MG cells transfected different CLK1 siRNAs. All three CLK1 siRNAs showed a reduction in the amount of FUS in the cell, with CLK1_1 and CLK1_5 having a greater effect on the level of FUS present in the cell.

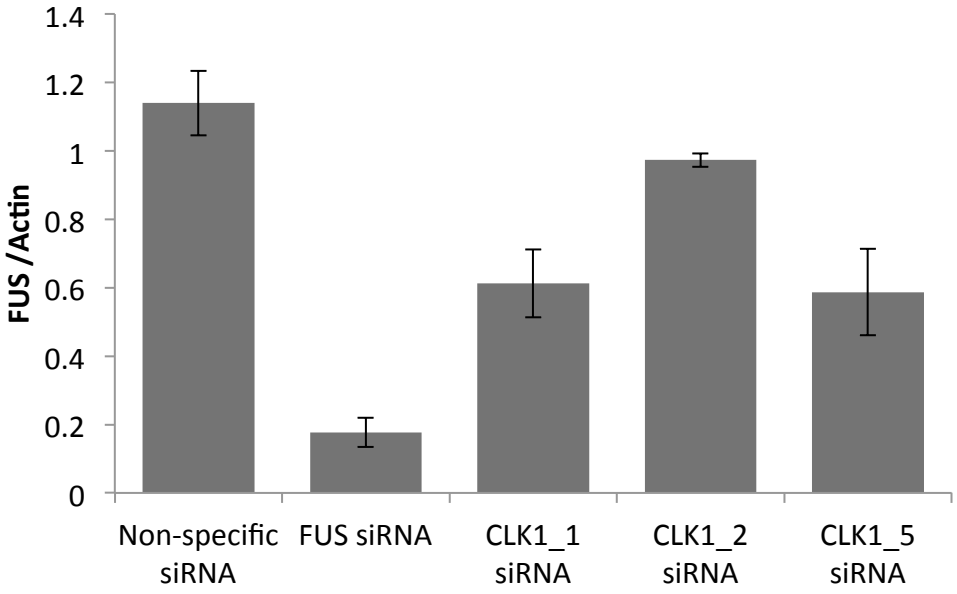
1.4
1.2
1
0.8
0.6
0.4
0.2
0
FUS /Actin
Non-specific siRNA
FUS siRNA
CLK1_1 siRNA
CLK1_2 siRNA
CLK1_5 siRNA

3.5.2. Serine and tyrosine phosphorylation on FUS

CLK1 has demonstrated to affect the localization and quantity of FUS *in vivo*. We hypothesized that it is responsible for those observed changes through post-translational modification of FUS. To determine if CLK1 is responsible for the phosphorylation of tyrosine and serine residues on FUS, lysates from cells transfected with convoluted CLK1 siRNAs was immunoprecipitated with anti-phosphotyrosine or anti-phosphoserine antibody and stained for FUS **Figure 14**. No FUS staining was observed in cells lysates from cells transfected with FUS siRNA. FUS was present in cells transfected with CLK1 siRNA. However, no FUS was immunoprecipiated with anti-phosphoserine or tyrosine antibodies from these cell lysates. The absence of FUS immunoprecipitated with phospho-antibodies in cells treated with CLK1 siRNA is consistent with the prospect that CLK1 is involved in the post-translational modification of FUS.

Figure 14. Western blot of U87MG cells transfected with non-specific, FUS, or CLK1 siRNAs.

The left column indicates the specific protein detected for on the blot. The top row indicates which siRNA the lysates were transfected with. In the bottom two rows, cell lysates were immunoprecipitated with either phosphoserine or tyrosine antibodies and stained for FUS. No FUS staining was observed in cells transfected with FUS or CLK1 siRNAs immunoprecipitated with anti-phosphoserine or tyrosine antibodies.

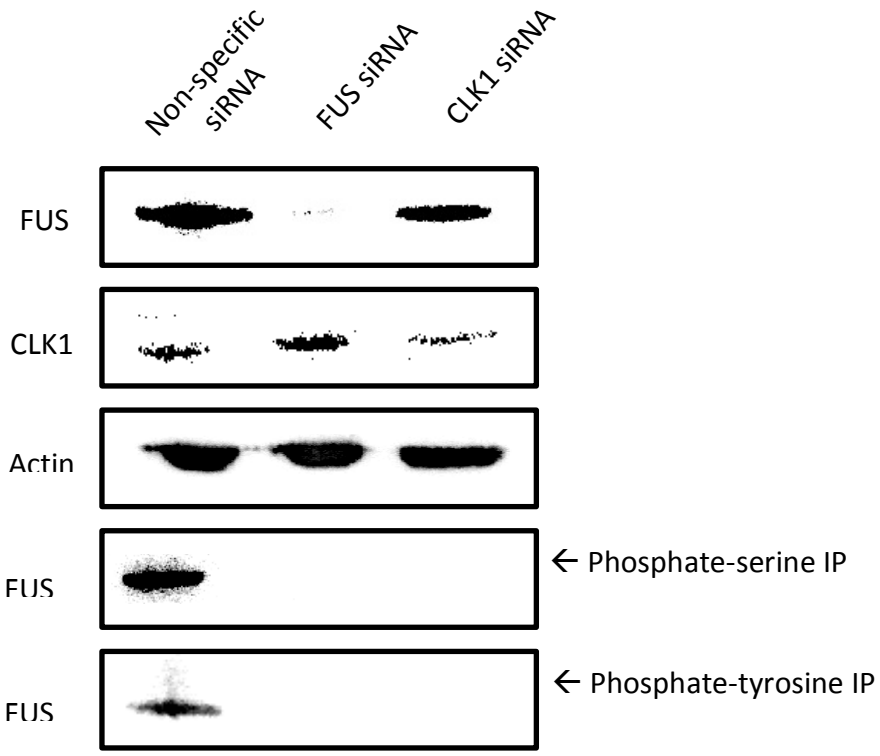
Non-specific siRNA
FUS siRNA
CLK1 siRNA
FUS
CLK1
Actin
FUS
← Phosphate-serine IP
FUS
← Phosphate-tyrosine IP

3.5.3. In vitro kinase assay

In vitro kinase assay was performed with CLK1 and truncated FUS. CLK1 served as an internal control, because it is an autophosphorylation kinase **Figure 15**. CLK1 was combined with non-mutated or mutated FUS isoforms, Fus3 or Fus3F. The terminal tyrosine on Fus3F fragment is mutated to a phenylalanine. The substitution of the terminal tyrosine to phenylalanine increases the phosphorylation state of FUS by CLK1. In other words, CLK1 more efficiently phosphorylates the mutant isoform in comparison to the wild type form of FUS. The vitro kinase indicates CLK1 can phosphorylate FUS, and the terminal tyrosine somehow influences this activity.

Figure 15. *In vitro* kinase assay with CLK1 and truncated FUS.

Fus3F is a mutated form of Fus3 where phenylalanine is substituted for the terminal tyrosine. Fus3F has a greater degree of phosphorylation by CLK1 in comparison to Fus3.

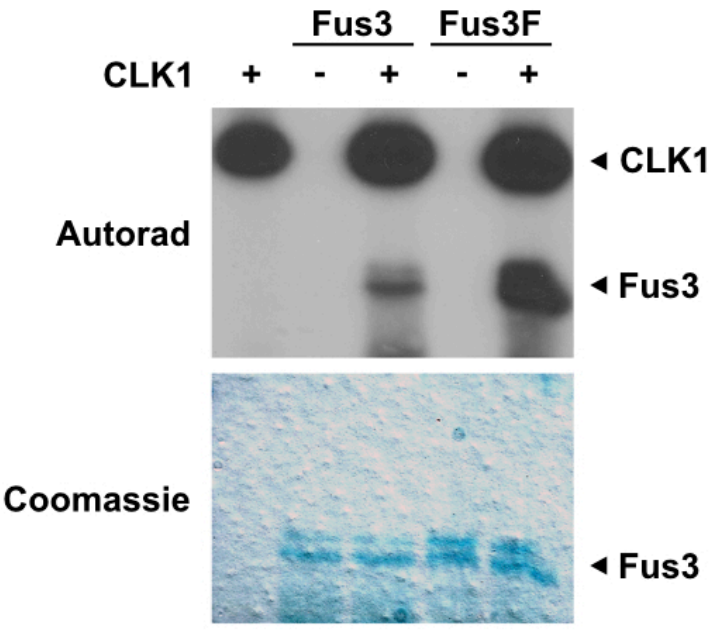
Fus3
Fus3F
CLK1
+
-
+
-
+
Autorad
CLK1
Fus3
Coomassie
Fus3

Chapter 4 Discussion

In this work, we conducted a kinome-wide RNAi screen focused on FUS, and identified several candidates that could potentially post-transnationally modify FUS and change its nuclear localization. Among them are MAPK1 and CLK1. Since CLK1 and FUS share similar functions and are both involved in RNA metabolism, the role of CLK1 became a particular interest to us. We elected to validate the involvement CLK1 in the post-translational modification of FUS. We demonstrated that CLK1 affects the subcellular localization of FUS from the nucleus into the cytoplasm, and CLK1 does in fact phosphorylate serine and tyrosine residues on FUS *in vitro*.

Majority of the FUS ALS causative mutations are located at the highly conserved C-terminus, which makes the post-translational modification of the C-terminus of particular interest to us. C-terminus of FUS is involved in RNA binding and contains the non-classical proline-tyrosine nuclear localization signal (Mackenzie et al., 2010). Phosphorylation of tyrosine residues in NLS in proteins often induces critical structural changes for function/recognition, and most importantly subcellular localization; as shown in FUS homologues, Sam68 and EWS. The post-translational modification of amino acids in the C-terminal sequences as shown in Sam68 and EWS suggest that the post-translational modification of FUS at the similar region could be crucial to the localization of FUS.

We hypothesize that the post-translational modification of FUS amino acids at the C-terminus is crucial to its subcellular localization and function.

Since the implication of FUS in ALS is a recent identification and only a few binding partners of FUS are known, we approached the project by conducting a kinome-wide RNAi screen. The kinase screen has provided us with a large amount of valuable information that require further analysis and verifications to unravel the mystery surrounding the involvement of FUS in ALS.

4.1 Kinome Screen

We examined the bank of cell lines available at the institutes based on a series of criteria such as morphology, and endogenous level of FUS expression. The selected ones were IF stained for FUS, among them were U87MG, U2OS. We chose to use U87MG for the kinome screen because the cells displayed strong FUS IF staining at a high dilution of the antibodies, flat morphology, and adhered strong enough to the plates to endure the washes involved in the procedures. U87MG has a large cytoplasm that was suitable for measuring and visually monitoring the translocation of FUS between the nucleus and the cytoplasm.

The process of optimizing the screen (to use U87MG in 384-well plates) took over six months. The period is much longer than the planned two-month. This occurred because we selected the wrong protocol to optimize. The said protocol was intended for antibodies with significantly stronger binding affinity than ours. We found the correct

protocol after identifying the problem. The screening process was further delayed when we attempted to create a stronger positive control, M9M peptide inhibitor, than Trn1. The intent was to achieve a stronger Z-prime factor, which would have allowed for better positive hits identification. The transduction of the M9M peptide inhibitor into the U87MG cells caused significant cell death; therefore, it was deemed unsuitable for the screen. We decided to pursue the kinome screen with the original Trn siRNA as the positive control, and the non-specific siRNA for the negative control. Together they obtained a Z-prime factor of 0.7, which was within the optimal 0.5-1.0 value range, indicating a statistically significant difference between the positive and negative controls and allowed us to proceed to conduct the screen.

The data from the Opera imaging system was uploaded into software named Columbus. We optimized the algorithm within the program to: recognize individual cells, to mark the nucleus and cytoplasm, and to measure the FUS intensity in each subcellular compartment of the individual cells. All kinases in the screen were analyzed for cell number, FUS intensity in the nucleus and the cytoplasm. First, kinases with significant cell death were eliminated, since the functions of these kinases were most likely to be essential to cell survival. Second, a nuclear-to-cytoplasmic FUS intensity ratio was calculated for the remaining kinases. Kinases within the range of the non-specific siRNA values were removed from further consideration because they were deemed statistically in affect the localization of FUS. Thirdly, we inspected the images from the screen to eliminate glare or other issues that could have occurred in capturing the wells.

Then we researched the function of the remaining kinases. There were a number of different kinases available for us to further pursue testing with. In the end, we selected CLK1 because there was a significant reduction in the nuclear FUS accompanied by an increase of the cytoplasmic FUS levels in a pattern similar to the Trn1 positive control.

4.2 CLK1

CLK is a part of the CDC2-like family. The CLK family consists of four isoforms: CLK1, CLK2, CLK3, and CLK4. All four isoforms bind and phosphorylate splicing factors, but they have target molecules. The effects of CLK2, CLK3, and CLK4 on subcellular localization of FUS were analyzed but they were not statistically significant to be pursued further in the study. CLK1 was first identified and intensely studied by Dr. John Bell at the Ottawa Hospital Research Institute in the 1990's. In 1991, the protein was first identified in rodents as a LAMMER kinase that regulates cell growth and differentiation (Howell et al., 1991). Four years later, the same lab demonstrated that CLK1 functions as a dual specific kinase that phosphorylates serine/threonine and tyrosine residues in mammalian cells (Duncan et al., 1995).

In this study, we have demonstrated FUS as one of its targets. Also, CLK1 binds and phosphorylates serine/arginine rich mRNA splicing factors, such as SRSF1, SRSF3, and PTPN1. Prasad et al. demonstrated the overexpression CLK1 *in vivo* resulted in subcellular redistribution of serine-arginine proteins and altered mRNA splicing (Prasad et al., 1999). Similar to FUS, CLK1 is also involved in RNA metabolism, it also self

regulates and maintains homeostasis by splicing its own mRNA according to the level of kinase activity.

In the kinome screen, CLK1 knock down had a statistically significant decrease in nuclear-to-cytoplasmic FUS ratio, where the cytoplasm had a greater increase in FUS intensity than the nucleus. When the cells were grouped based on nuclear FUS intensity on a histogram, CLK1 knock down cells had a distribution pattern similar to the positive control where majority of the cells had decreased nuclear FUS intensity. In contrast, the negative control shifted to a higher value. Furthermore, the IF images showed CLK1 knocked down cells had a larger cytoplasm similar to the positive control. The data strongly suggests that CLK1 induced FUS subcellular translocation, possibly through post-translational modification of FUS.

To validate our findings, the mixture of four siRNAs targeting CLK1 in the kinome screen was deconvoluted and the individual effect of each siRNA on FUS localization was studied. Interestingly, the CLK1 siRNAs had varying effects. CLK1_1, and CLK1_5 reduced nuclear-to-cytoplasmic FUS intensity and total amount of FUS. CLK1_2 performed the opposite by increasing the nuclear-to-cytoplasmic FUS intensity. CLK1_6 had minimal influence on the FUS subcellular localization. We suspect the variations in targeting efficiency and extents of off-target effect among the siRNAs are accountable for the varying results observed with the deconvoluted siRNAs.

Early in the study, CLK1_2 appeared to have a similar effect as CLK1_1 but to a greater extent (though later research proved otherwise). We proceeded to design a primer for the site-directed mutagenesis for CLK1_2, in which we aimed to modify nucleotides targeted by CLK1_2 to verify the siRNA specificity. However, the targeted region had a high GC content and necessitated higher melting point for the primers than allowed by the procedure. We were not able to successfully pursue the mutagenesis experiment. We pursued the remaining validation process using convoluted siRNA. We performed immunoprecipitation with anti-phosphate antibodies, and stained for FUS on the western blot. We were very excited to observe that there was a lack of FUS staining in the CLK1 siRNA transfected cell. This evidence is consistent with the contingency that CLK1 is responsible for the phosphorylation of serine and tyrosine amino acids on FUS protein.

To further endorse our findings, we performed *in vitro* kinase assay with FUS truncates and CLK1. CLK1 phosphorylated both wild-type and mutated forms, but it more efficiently phosphorylated the mutant isoform where the terminal tyrosine was substitute to a phenylalanine. This however excludes any possibility that the phosphorylation site is the terminal tyrosine. We postulate that the terminal tyrosine substitution of with phenylalanine modified the protein structure that promoted the phosphorylation of internal sites.

Cytoplasmic protein aggregation is the hallmark of ALS. In ALS, FUS is trapped in cytoplasmic inclusions, which hinders FUS from transporting mRNA to the dendritic spines. This lack of site-specific protein translocation contributes to the changes in neuron morphology and function. The exact function and regulation of FUS is still being elucidated. In this study, we demonstrated that in U87MG cells transfected with CLK1 siRNA, wild-type FUS was hypophosphorylated and formed aggregates in the cytoplasm corresponding to a decreased nuclear-to-cytoplasm ratio. Future studies elucidating the specific sites on FUS modified by CLK1 will expand our understanding on the mechanism of interaction and the involvement of FUS in the ALS pathology.

4.3 Summary

In this study, we provided data that is consistent with the contingency that CLK1 is responsible for the phosphorylation of serine and tyrosine residues in FUS. The post-translation modification effectively changed the localization of FUS in the nucleus. The increased level of phosphorylation in FUS Y526F in comparison to the wild-type provides a potential explanation for the FUS found in the intraneuronal cytoplasmic aggregates in affected ALS patients. The identification of CLK1 as FUS-modifying kinase is consistent with roles ascribed to both in the binding and regulation of RNA. Aside from CLK1, the kinome-wide RNAi screen has provided a large amount of data that should be further analyzed to identify the relationship of the other kinases relevant to FUS. This information could shed light on the function and interaction of the protein and be critical to gaining further understanding of the FUS pathology and its involvement in ALS.

References

1. Al-Chalabi, A., et al. 2012. The genetics and neuropathology of amyotrophic lateral sclerosis. Acta neuropathologica. 124: 339-52.

2. Ben-David Y., Letwin K., Tannock L., Bernstein A., Pawson T. A mammalian protein kinase with potential for serine/threonine and tyrosine phosphorylation is related to cell cycle regulators. (1991) EMBO J. 10, 317–325.

3. Boillee S, Yamanaka K, Lobsiger CS, Copeland NG, Jenkins NA, Kassiotis G, et al. 2006. Onest and progression in inherited ALS determined by motor neurons and microglia. Science 312:1389-92.

4. Bosco DA, Morfini G, Karabacak NM et al. 2010. Wild-type and mutant SOD1 share an aberrant conformation and a common pathogenic pathway in ALS. Nat Neurosci 13:1396–1403.

5. Buratti E, Doerk T, Zuccato E, Pagani F, Romano M, Baralle FE. 2001. Nculear factor TDP-43 and SR proteins promote in virtro and in vivo CFTR exon 9 skipping. EMBO J 20:1774-1784.

6. Byrne, S. Hardiman O. 2010. Familial aggregation in amyotrophic lateral sclerosis. Annals of neurology. 67: 554.

7. Chiang, P.M., et al. (2010)Deletion of TDP-43 down-regulates Tbc1d1, a gene linked to obesity,and alters body fat metabolism. Proceedings of the National Academy of Sciences of the United States of America. 107(37):16320-4.

8. Crow JP, Sampson JB, Zhuang Y, Thompson JA, Beckman JS. 1997. Decreased zinc affinity of amyotrophic lateral sclerosis-associated superoxide dismutase mutants leads to enhanced catalysis of tyrosine nitration by peroxynitrite. J Neurochem 69:1936–1944.

9. Deng Q., Holler C., Taylor G., Hudson K., Watkins W., Gearing M., Ito D., Murray M., Dickson D., Seyfried N., Kukar T. FUS is Phosphorylated by DNA-PK and Accumulates in the Cytoplasm after DNA Damage. (2014). J. Neurosci. 34(23), 7802-7813

10. Dormann D, Rodde R, Edbauer D, Bentmann E, Fischer I, Hruscha A, Than ME, Mackenzie IRA, Capell A, Scmid B, Neumann M, Haass C. 2010. ALS-associated fused in sarcoma (FUS) mutations disrupt transportin-mediated nuclear import. EMBO J 29: 2841-2857.

11. Duncan P., Howell B., Marius R., Drmanic S., Douville E., and Bell J. Alternative Splicing of STY, a Nuclear Dual Specificity Kinase. (1995) J. Bio. Chem. 270, 21524-21531.

12. Fujii R, Okabe S, Urushido T, Inoue K, Yoshimura A, Tachibana T, Nishikawa T, Hicks GG, Takumi T. 2005. The RNA binding protein TLS is translocated to dendritic spines by mGluR5 activation and regulates spine morphology. Curr Biol. 15(6):587-93.

13. Fujii R, Takumi T. December 2005. TLS facilitates transport of mRNA encoding an actin-stabilizing protein to dendritic spines. J. Cell. Sci. 118 (Pt 24): 5755–65.

14. Gitcho MA, Baloh RH, Chakraverty S et al. 2008. TDP-43 A315T mutation in familial motor neuron disease. Ann Neurol 63:535–538.

15. Gurney M, Pu H, Chiu A et al. 1994. Motor neuron degeneration in mice that express a human Cu, Zn superoxide dismutase mutation. Science 264:1772–1775.

16. Higdon R, Stewart E, Stanberry L, Haynes W, Choiniere J, Montague E, Anderson N, Yandl G, Janko I, Broomall W, Fishilevich S, Lancet D, Kolker N, Kolker E. 2013. MOPED enables discoveries through consistently processed proteomics data. Journal of proteome research. 13: 107-113.

17. Hornbeck PV, Kornhauser JM, Tkachev S, Zhang B, Skrzypek E, Murray B, Latham V, Sullivan M (2012) PhosphoSitePlus: a comprehensive resource for investigating the structure and function of experimentally determined post-translational modifications in man and mouse. Nucleic Acids Res. 40(Database issue), D261–70..do;jsessionid=48332DF629BA4B2D9CB018A315D6BC82

18. Howell B. W., Afar D. E. H., Lew J., Douville E. M. J., Icely P. L. E., Gray D. A., Bell J. C. STY, a tyrosine-phosphorylating enzyme with sequence homology to serine/threonine kinases. (1991) Mol. Cell. Biol. 11, 568–572.

19. Iguchi Y., Katsuno M., Ikenaka K. Amyotrophic lateral sclerosis: an update on recent genetic insights. (2013) J. Neurol. 26, 2917-2927.

20. Ishidate T, Yoshihara S, Kawasaki Y, Roy BC, Toyoshima K and Akiyama T. 1997. Identification of a novel nuclear localization signal in Sam68. FEBS Letters. 409:237 -241.

21. Ishidate, T., Yoshihara, S., Kawasaki, Y., Roy, B. C., Toyoshima, K., and Akiyama, T. (1997) FEBS Lett. 409, 237-241

22. Joyce, PI, et al. 2011. SOD1 and TDP-43 animal models of amyotrophic lateral sclerosis: recent advances in understanding disease toward the development of

clinical treatments. Mammalian genome : official journal of the International Mammalian Genome Society. 22(7-8):420-48.

23. Kolker E, Higdon R, Haynes W, Welch D, Broomall W, Lancet D, Stanberry L, and Kolker N. 2012. Model Organism Protein Expression Database. Nucleic Acids Res 40: D1093–1099.

24. Kovar H. 2011. Dr. Jekyll and Mr. Hyde: The two faces of the FUS/EWS/TAF15 protein family. Sarcoma 2011:837474.

25. Kovar H. 2011. Dr. Jekyll and Mr. Hyde: The two faces of the FUS/EWS/TAF15 protein family. Sarcoma: 837474.

26. Kwiatkowski TJ Jr, Bosco DA, LeClerc AL et al. 2009. Mutations in the FUS/TLS gene on chromosome 16 cause familial amyotrophic lateral sclerosis. Science 323:1205–1208.

27. Lagier-Tourenne, C. and D.W. Cleveland. 2009. Rethinking ALS: the FUS about TDP-43. Cell. 136: 1001-4.

28. Lee BJ, Cansizoglu AE, Süel KE, Louis TH, Zhang Z, Chook YM. 2006. Rules for nuclear localization sequence recognition by karyopherinβ2. Cell 126(3):543–558.

29. Leemann-Zakaryan RP, Pahlich S, Grossenbacher D, Gehring H. 2001. Tyrosine phosphorylation in the C-terminal nuclear localization and retention signal (C-NLS) of the EWS protein. Sarcoma 2011:218483.

30. Leigh PN, Dodson A, Swash M, Brion JP, Anderton BH. 1989. Cytoskeletal abnormalities in motor neuron disease. An immunocytochemical study. Brain J Neurol 112(Pt 2):521–535.

31. Ling, S.C., et al. 2010. ALS-associated mutations in TDP-43 increase its stability and promoteTDP-43 complexes with FUS/TLS. Proceedings of the National Academy of Sciences of the United States of America. 107(30): 13318-23.

32. Lukong KE, Larocque D, Tyner AL & Richard S. 2005. Tyrosine phosphorylation of sam68 by breast tumor kinase regulates intranuclear localization and cell cycle progression. Journal of Biological Chemistry. 280: 38639–38647.

33. Lukong KE, Larocque D, Tyner AL, Richard S. 2005. Tyrosine phosphorylation of Sam68 by breast tumor kinase regulates intranuclear localization and cell cycle progression. The Journal of Biological Chemistry 280(46):38639–38647.

34. Mackenzie I, Bigio E, Ince P et al. 2007. Pathological TDP-43 distinguishes sporadic amyotrophic lateral sclerosis from amyotrophic lateral sclerosis with SOD1 mutations. Ann Neurol 61:427–434.

35. Mackenzie, I.R., R. Rademakers, and M. Neumann. 2010. TDP-43 and FUS in amyotrophic lateral sclerosis and frontotemporal dementia. Lancet neurology. 9: 995-1007.

36. Menzies, F.M., et al. 2002. Mitochondrial dysfunction in a cell culture model of familial amyotrophic lateral sclerosis. Brain : a journal of neurology. 125: 1522-33.

37. Mitchell JC, McGoldrick P, Vance C, Hortobagyi T, Sreedharan J, Rogelj B, Tudor EL, Smith BN, Klasen C, Miller CC, Cooper JD, Greensmith L, Shaw CE. 2013. Overexpression of human wild-type FUS causes progressive motor neuron degeneration in an age- and dose-dependent fashion.Acta Neuropathol. 125(2):273-88.

38. Nagai M, Re DB, Nagata T et al. 2007. Astrocytes expressing ALS-linked mutated SOD1 release factors selectively toxic to motor neurons. Nat Neurosci 10:615–622.

39. Neumann M, Sampathu DM, Kwong LK et al. 2006. Ubiquitinated TDP-43 in frontotemporal lobar degeneration and amyotrophic lateral sclerosis. Science 314:130–133.

40. Niu C, Zhang J, Gao F, Yang L, Jia M, Zhu H, Gong W. 2012. FUS-NLS/Transportin 1 Complex Structure Provides Insights into the Nuclear Targeting Mechanism of FUS and the Implications in ALS. PLOS. 10.1371.

41. Niu C1, Zhang J, Gao F, Yang L, Jia M, Zhu H, Gong W. 2012. FUS-NLS/Transportin 1 complex structure provides insights into the nuclear targeting mechanism of FUS and the implications in ALS. PLoS One 7:e47056.

42. Niwa J-I, Yamada S-I, Ishigaki S et al. 2007. Disulfide bond mediates aggregation, toxicity, and ubiquitylation of familial amyotrophic lateral sclerosis-linked mutant SOD1. J Biol Chem 282:28087–28095.

43. Ou SH, Wu F, Harrich D, García-Martínez LF, Gaynor RB. 1995. Cloning and characterization of a novel cellular protein, TDP-43, that binds to human immunodeficiency virus type 1 TAR DNA sequence motifs. Journal of Virology 69 (6): 3584–96.

44. Pasinelli P, Brown RH. 2006. Molecular biology of amyotrophic lateral sclerosis: insights from genetics. Nat Rev Neurosci 7:710–723.

45. Polymenidou, M., et al. 2011. Long pre-mRNA depletion and RNA missplicing contribute to neuronal vulnerability from loss of TDP-43. Nat Neurosci. 14(4): 459-68.

46. Prasad J., Colwill K., Pawson T., Manley1 J. 1999. The Protein Kinase Clk/Sty Directly Modulates SR Protein Activity: Both Hyper- and Hypophosphorylation Inhibit Splicing. Mol. Cell Biol. 19(10), 6991-7000.

47. Renton, A.E. State of play in amyotrophic lateral sclerosis genetics.(2014) Nature Neurosci.17.1, 17-23

48. Rosen DR, Siddique T, Patterson D et al. 1993. Mutations in Cu/Zn superoxide dismutase gene are associated with familial amyotrophic lateral sclerosis. Nature 362:59–62.

49. Rowland L.P., Stern Y. 2006. An observational study ofcognitive impairment in amyotrophic lateral sclerosis. Arch. Neurol. 63: 345-352.

50. Rowland, LP. 2001. How amyotrophic lateral sclerosis got its name: the clinical-pathologic genius of Jean-Martin Charcot. Arch. Neurol. 58:512–515.

51. Schaab C, Geiger T, Stoehr G, Cox J, Mann M. 2012. Analysis of high-accuracy, quantitative proteomics data in the MaxQB database. Mol Cell Proteomics 11.

52. Sephton, C.F., et al. 2010. TDP-43 is a developmentally regulated protein essential for earlyembryonic development. Journal of biological chemistry. 285(9):6826-34.

53. Sreedharan J, Blair IP, Tripathi VB et al. 2008. TDP-43 mutations in familial and sporadic amyotrophic lateral sclerosis. Science 319:1668–1672.

54. Valdmanis PNB, Rouleau GAMDP. 2008. Genetics of familial amyotrophic lateral sclerosis. Neurology 70:144–152.

55. Van Deerlin VM, Leverenz JB, Bekris LM et al. 2008. TARDBP mutations in amyotrophic lateral sclerosis with TDP-43 neuropathology: a genetic and histopathological analysis. Lancet Neurol 7:409–416.

56. Van Deerlin VM, Leverenz JB, Bekris LM, Bird TD, Yuan W, Elman LB, Clay D, Wood EM, Chen Plotkin AS, Martinez-Lage M, Steinbart E, McCluskey L, Grossman M, Neumann M, Wu IL, Yang WS, Kalb R, Galasko DR, Montine TJ, Trojanowski JQ, Lee VM, Schellenberg GD, Yu CE. 2008. TARDBP mutations in amyotrophic lateral sclerosis with TDP-43 neuropathology: a genetic and histopathological analysis. Lancet Neurol. 7(5):409-16.

57. Van Langenhove T, van der Zee J, Sleegers K, Engelborghs S, Vandenberghe R, Gijselinck I, Van den Broeck M, Mattheijssens M, Peeters K, De Deyn PP, Cruts M, Van Broeckhoven C. 2010. Genetic contribution of FUS to frontotemporal lobar degeneration. Neurology. 74(5):366-71.

58. Vance C, Rogelj B, Hortobagyi T, De Vos KJ, Nishimura AL, Sreedharan J, Hu X, Smith B, Ruddy D, Wright P, Ganesalingam J, Williams KL, Tripathi V, Al-Saraj S, Al-Chalabi A, Leigh PN, Blair IP, Nicholson G, de Belleroche J, Gallo JM, Miller CC, Shaw CE. Mutations in FUS, an RNA processing protein, cause familial amyotrophic lateral sclerosis type 6. Science. 2009;323(5918):1208–11.

59. Wang M., Weiss M., Simonovic M., Haertinger G., Schrimpf S.P., Hengartner M.O., von Mering C.PaxDb, a database of protein abundance averages across all three domains of life.(2012) Mol. Cell Proteomics. 8, 492-500

60. Wu, L.S., et al. 2010. TDP-43, a neuro-pathosignature factor, is essential for early mouse embryogenesis. Genesis. 48(1): 56-62.

61. Yokoseki A, Shiga A, Tan CF, Tagawa A, Kaneko H, Koyama A, Eguchi H, Tsujino A, Ikeuchi T, Kakita A, Okamoto K, Nishizawa M, Takahashi H, Onodera O. 2008. TDP-43 mutation in familial amyotrophic lateral sclerosis.Ann Neurol. 63:538-42.

62. Zhou Y, Liu S, Öztürk A, Hicks G. 2014. FUS-regulated RNA metabolism and DNA damage repair. Rare Diseases. 2: e29515.

Contributions of collaborators

The RNAi kinome screen was completed at Dr. Robert Screaton Lab, Children's Hospital of Eastern Ontario Research Institute.

Dr. Luc Sabourin Lab, The Ottawa Hospital Research Institute, performed the in vitro kinase assay.

Curriculum vitae

Serena Esmée Blythe Liu

Education

2014-2018 **Doctor of Medicine (M.D.)**
Wayne State University School of Medicine

2012-2014 **M.Sc. in Biochemistry**
University of Ottawa
Thesis: Kinome-wide RNAi screening to identify kinases involved in post-translational modification of FUS
Supervisors: Dr. Douglas Gray

2009 **International Summer Exchange Program**
University of Ulm

2008-2012 **B.Sc. Hons. Major in Biochemistry, Minor in German Studies Certificate in International Studies**
Queen's University
Top 3% of the degree program

Scholarships

2015 Robert C. Fraser, M.D., Scholarship

2012-2014 QEIIGSST scholarship - $30,000

2012-14 University of Ottawa Excellence Scholarship

Conference abstracts

Liu SEB, Du Q, Screaton R, Woulfe J, Gray DA. 2015. Kinome-wide RNAi screening to identify kinases involved in post-translational modification of FUS. China-Canada Symposium on Systems Biology, Shanghai. (Poster)

Liu SEB, Du Q, Screaton R, Woulfe J, Gray DA. 2014. Kinome-wide RNAi screening to identify kinases involved in post-translational modification of FUS. Medical Student Research Symposium, Detroit. (Oral Presentation)

Academic work

2014	Teaching Assistant Introduction to Biochemistry University of Ottawa
2009	Laboratory Research Assistant Queen's University Supervisor: Dr. Haiyan Chu